ANALYSIS OF SOLAR PANEL EFFICIENCY THROUGH COMPUTATION AND SIMULATION

Hongyu Guo, University of Houston-Victoria; Mehrube Mehrubeoglu, Texas A&M University-Corpus Christi

Abstract

Solar panels are known to have low efficiency, typically less than 25%. And combined with a solar panel orientation that is not optimized for the direction of the incident sun, the efficiency is further reduced. In this study, a computational and visual model was developed for the apparent diurnal motion of the sun to determine the declination and azimuthal angles at which a solar panel should be oriented at any time on any day for active solar trackers to maximize the received solar irradiance at any location on earth. A software simulation tool was developed to compute sunrise time, sunset time, and duration of daytime for any latitude using a geocentric model. The efficiency of solar panels due to incident angles was defined and analyzed for reduced-degree-of-freedom solar tracking systems. The analysis has significance in providing guidance in the decision process of initial solar panel investment and installation regarding the trade-offs between efficiency and cost.

Introduction

Solar panels have efficiencies lower than 40% and most typically less than 25% [1]. Many factors contribute to this low efficiency, including solar panel technology, materials and charging process. Orientation of the solar panel is one of the major factors contributing to solar energy conversion efficiency. In this study, the authors focused on the orientation of solar panels to maximize received solar irradiation to improve energy conversion based on the received solar energy.

Depending on the nature of the application and the cost requirements, the orientation of the solar panel can be either fixed or movable. Fixed-orientation solar panels are the least expensive to install but they are also the least efficient. A simple improvement can be made by a rotatable solar panel on a single axis where the tilt angle is adjusted seasonally, or monthly. To make better use of the solar energy, some tracking systems are designed to minimize the incident angle of the sunlight onto the solar panel [2-7]. The sophistication of the tracking system depends on the trade-off between cost and efficiency. Single-axis as well as dual-axis trackers exist. A single-axis tracker can be designed as a horizontal single-axis tracker (HSAT), vertical single-axis tracker (VSAT), or tilted single-axis tracker (TSAT). Different types of dual-axis trackers have also been developed and depend on the choice of the primary and secondary axis. With different system drive methods, tracking can be active or passive. The goal of dual-axis trackers is to make the solar panel track the sun so that the sun's rays are always orthogonal to the solar panel.

A typical solar tracking method requires photoelectric detection that utilizes a photoelectric sensor to follow the sun; however, this method suffers from unpredictable weather conditions which could affect tracking of the sun. A weather-independent method involves solar trajectory tracking through mathematical computations [8]. Although papers on solar tracking have been published, none includes simulations for visualizations [8-11]. Numerical information on local sunrise, sunset time, and length of a day in a year at any latitudinal location is available in astronomical almanacs and online at institutions such as U.S. Naval Observatory; however, a useful computational and visualization model of these astronomical events to assist with solar panel orientation for maximum solar irradiance at any time, any day and any location was not found in the literature. Some groups have investigated monthly solar panel orientation strategies [12]. The solar panel efficiency affected by the orientation is of interest in multiple applications [13-15].

In this study, a geocentric model was developed for computation and visualizations of the apparent diurnal motion of the sun and to simulate the computed orientation of an active dual-axis solar panel tracking system. Simulations of the apparent diurnal motion of the sun can be used to drive the dual-axis solar tracker. Snapshots of the diurnal motion of the sun for a sample date are shown in Figure 1. Duration of daytime and nighttime plots for various latitudes are displayed. MATLAB programs were developed for this simulation and visualization. In practical applications of solar panels, to reduce the cost of the installation, a reduced-degree-of-freedom solar tracking system is often adopted. These systems include seasonally adjusted fixed solar panels and single-axis solar trackers. The efficiency due to incident angles of these reduced-degree-of-freedom solar tracking systems is defined and investigated. This analysis has significance in practice for engineers who make decisions on the trade-offs between efficiency and cost in the initial planning stage of investment and installation.

Solar Tracking by Computing the Solar Declination and Azimuthal Angles

A simple model can be used to compute and simulate solar tracking. For the precision requirement of solar tracking, it is enough to assume that the orbit of the earth is a circle. It is more convenient, however, to use a geocentric model than a heliocentric model. It is necessary to understand the relationship between the horizon plane and the plane depicting the diurnal motion of the sun to see how the sun's location and orbit affects sunrise time, sunset time, and the duration of daytime and nighttime, and in effect how the solar panel should be oriented. Geometric equations relating the duration of daytime and nighttime to the relative position of the sun to the equatorial plane and the horizon plane are derived below.

Solar Declination on Any Date throughout the Year

The celestial sphere is shown in Figure 1, where the earth is at the center. N is the celestial North Pole. If the observer is standing at a point on earth with latitude, λ , then the great circle in the x-y plane in the Cartesian coordinate system with points S, B, R, and A is the local horizon circle. The great circle with points E, L, B, N, Z, H, Q, and A is the local meridian. This circle is in the y-z plane.

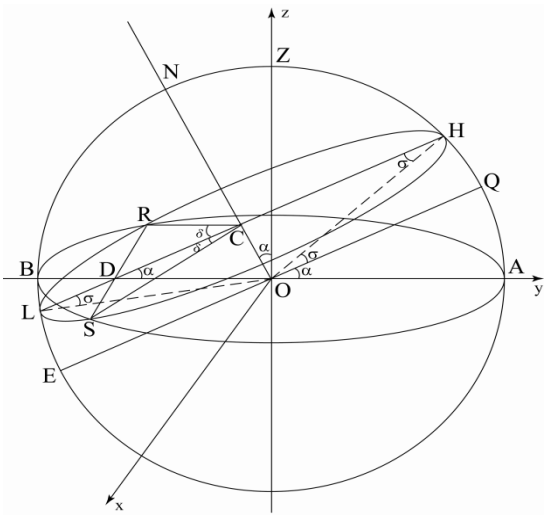

Figure 1. Diurnal Motion of the Sun on the Celestial Sphere

The line EQ is the diameter of the celestial sphere, which is also in the equatorial plane. (The equatorial plane is omitted in Figure 1 for clarity.) ON is the axis of the celestial sphere. ON is perpendicular to EQ. The small circle with points H, R, L, and S is the diurnal path of the sun. C is the center of this small circle. R is the point of sunrise, whereas S is the point of sunset. H marks the position of the sun at noon, and L is the position of the sun at midnight. The arc RHS represents the daytime path, and the arc SLR represents the nighttime path of the sun. LCH is a diameter of that small circle (CR, CL, CS, and CH are radii of the same circle)**.** The plane of that small circle lies parallel to the equatorial plane and perpendicular to the axis ON. Hence, LH is parallel to EQ and LH is perpendicular to ON. Assume the radius of the celestial sphere is 1.

$\angle$ ZOQ = λ is the local latitude. Denote

$$\alpha = \frac{\pi}{2} - \lambda \tag{1}$$

as the co-latitude. In Figure 1,

$$\angle QOA = \angle CDO = \alpha \tag{2}$$

The solar declination is denoted by

$$\sigma = \angle HOQ \tag{3}$$

which is the angle from the sun at noon to the equatorial plane. σ changes throughout the year with a period of one year. At the vernal equinox, the sun is on the equator. H coincides with Q, and $\sigma = 0$. The angle between the ecliptic plane and the equatorial plane is called the obliquity of the ecliptic, with a value $\varepsilon = 23.5^{\circ}$. At the summer solstice, the sun is the highest in the sky and $\sigma = \varepsilon$, which has the maximum value. Figure 1 displays the diurnal path of the sun for an arbitrary day in the year, with a generic value of and $\sigma \neq \varepsilon$, . The obliquity of the ecliptic ε is not shown in Figure 1. At the autumnal equinox, the sun is on the equator again. H coincides with Q once again, and $\sigma = 0$. At the winter solstice, the sun is the lowest in the sky and $\sigma = -\varepsilon$, which is the minimum value.

The solar declination σ for any particular day in the year can be found, hence, the duration of daytime and nighttime can be computed for any latitude on earth and any day in the year.

Let θ denote the ecliptic longitude (not shown in Figure 1). θ varies from 0 to 2π when the sun moves on the ecliptic circle on the celestial sphere in one year. At vernal equinox $\theta = 0$; at summer solstice $\theta = \pi/2$; at autumnal equinox $\theta = \pi$; and at winter solstice $\theta = 3\pi/2$. The altitude of the sun

projected above the equatorial plane can be expressed as $\sin\theta\sin\varepsilon$. On the other hand, the same altitude is equal to $\sin\sigma$ in terms of the solar declination σ. By equating these two,

$$\sin\sigma = \sin\theta\sin\varepsilon \tag{4}$$

the solar declination σ can be found in terms of ecliptic longitude θ. When using the approximation of a circular orbit of the earth around the sun, θ can be assumed to change with a uniform angular velocity in the year. Let Y = 365.24 be the number of days in a year and let D be the number of days of the date of concern counting from vernal equinox. Then θ and D are simply related by

$$\theta = 2\pi D / Y \tag{5}$$

From Equations (4) and (5),

$$\sigma = \sin^{-1}(\sin\varepsilon\sin\theta) = \sin^{-1}(\sin\varepsilon\sin(2\pi D / Y)) \tag{6}$$

The solar panel should be oriented with an angle $\lambda + \sigma$ from the horizontal plane, which is the altitude of the sun at local noon.

Sunrise, Sunset and Duration of Daylight

The azimuthal rotation of the solar panel should follow the sun from sunrise to sunset. In Figure 1, the radius r of the small circle can be found by

$$r = \overline{CL} = \overline{CH} = \overline{CR} = \overline{CS} = \cos\sigma \tag{7}$$

Also,

$$\overline{CD} = \overline{OC}\cdot\cot\alpha = \sin\sigma\cdot\cot\alpha = \sin\sigma\cdot\tan\lambda \tag{8}$$

Since $\overline{CR} = \overline{CS}$, and $\overline{CD}$ bisects the angle $\angle RCS$, using Equations (7) and (8), the following Equation 9 is obtained:

$$\cos\delta = \frac{\overline{CD}}{\overline{CR}} = \frac{\sin\sigma\cdot\tan\lambda}{\cos\sigma} = \tan\sigma\cdot\tan\lambda \tag{9}$$

This yields

$$\delta = \cos^{-1}(\tan\sigma\cdot\tan\lambda) \tag{10}$$

The duration of the nighttime, n, is computed in hours as

$$n = 2\delta\cdot\frac{24}{2\pi} = \frac{24\delta}{\pi} \tag{11}$$

The duration of the daytime, d, is given in hours as

$$d = 24 - 24\delta/\pi = 24(1 - \delta/\pi)$$

Substituting for δ from Equation (10), d is obtained as

$$d = 24[1 - (\cos^{-1}(\tan\sigma.\tan\lambda))/\pi] \tag{12}$$

Using Equation (6), the duration of the daytime can be expressed as

$$d = 24 - \tfrac{24}{\pi}\cos^{-1}\{\tan\lambda\cdot\tan[\sin^{-1}(\sin\varepsilon\sin(2\pi D/Y))]\} \tag{13}$$

The sunrise time is then

$$T_r = 24\delta/2\pi$$

$$= (\tfrac{12}{\pi})\cos^{-1}\{\tan\lambda\cdot\tan[\sin^{-1}(\sin\varepsilon\sin(2\pi D/Y))]\} \tag{14}$$

and the sunset time is

$$T_s = 24 - T_r \tag{15}$$

in hours counting from midnight. All the times are local time for that particular longitude of the location of concern. The local time needs to be converted to standard time of the time zone where the location is in before they can be compared with published numerical data or observational data.

It is easy to check some special cases. When λ = 0. which is for a location on the equator, at any time during the year, d = 12, which means the daytime and nighttime are equal. If σ = 0, which is for the dates of the vernal equinox and autumnal equinox, then d = 12, which means the daytime and nighttime are equal for all different latitudes.

Computer Simulations

The algorithms for the diurnal motion of the sun and duration of daytime and nighttime were implemented in MATLAB based on the equations derived in the following section.

Diurnal Motion of the Sun

The diurnal motion and its plane for an arbitrarily chosen date, May 2, 2012, is shown in Figure 2 for different latitudes l. The software developed allows the user to choose any date and any latitude or location. Figure 2 shows the horizon plane (horizontal plane in all sub-figures) and the equatorial plane (plane parallel to the diurnal motion plane of the sun). The sphere represents the celestial sphere with the earth at its center. The small red ball represents the sun. Figure 2 can be validated with the appropriate values for latitude l and the solar declination s, based on the date of the

year described earlier. For example, for the date May 2, 2012, D = 42 (total number of days from vernal equinox March 21 to May 2) and s = 15.30° from Equation (6). For l = 90°, d = 0 (Equation (10)); then d = 24 hours, and n = 0 hours, as expected for the North Pole in summer. This is depicted in the top left subplot of Figure 2. Diurnal orbit of the sun is entirely above the horizon plane on the chosen date such that d = 24 hours for that day and n = 0, as expected for the North Pole. The bottom right subplot of Figure 2 is the diurnal path of the sun at l = -90 (South Pole) on May 2, 2012. Similarly, when l = 0, half of the diurnal orbit of the sun is above and the other half is below the horizon plane, suggesting equal day and night duration of 12 hours.

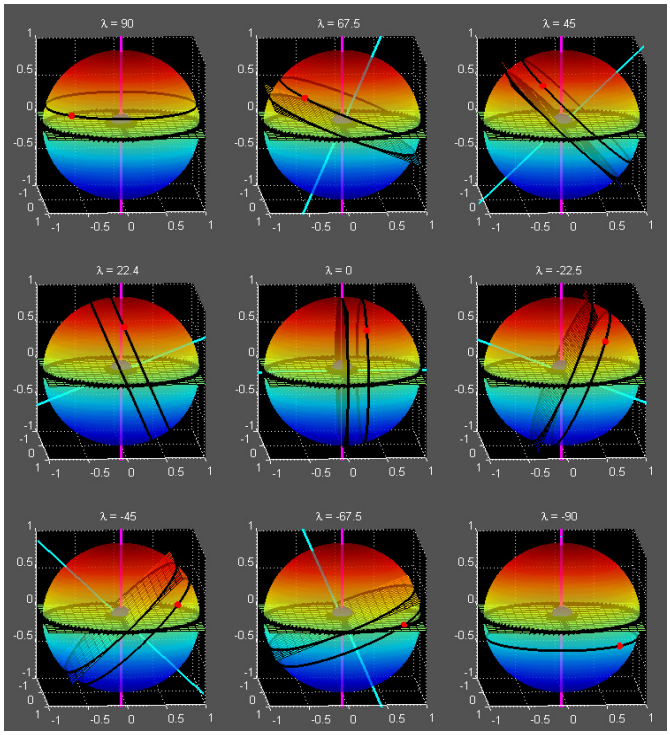

Figure 2. Computer Simulation of the Diurnal Motion of the Sun for May 2, 2012

Sunrise and sunset times for this date can be found from Equations (14) and (15), depending on the local latitude. Visual depiction of duration of daytime and nighttime for a given date is described in the next section.

Duration of Daytime for Any Latitude and Date

Figure 3 shows the duration of daytime and nighttime for one year for different latitudes l. Figure 3 was obtained by applying Equation (14) for each day of the year from January 1 to December 31. The duration of daytime on May 2, 2012, for a given l in Figure 3 (vertical green line) can be compared with the orbit of the sun on that day in Figure 2 in corresponding sub-figures. The comparison validates the results. Note, for example, for l = -45°, d = 9.88 hours and n = 14.12 hours, as depicted in Figure 3, bottom left subplot. These computations also match the depiction of daytime and nighttime durations in Figure 2 (bottom left), where the diurnal path of the sun is more below the horizon plane than it is above, visually validating the computations for May 2, 2012, with a longer nighttime than daytime. For this latitude, T_r = 7.06 hours after midnight, which is 7:04 AM and T_s = 16.94 hours, which is 4:56 PM. Notice that T_r and T_s represent local time instead of standard time.

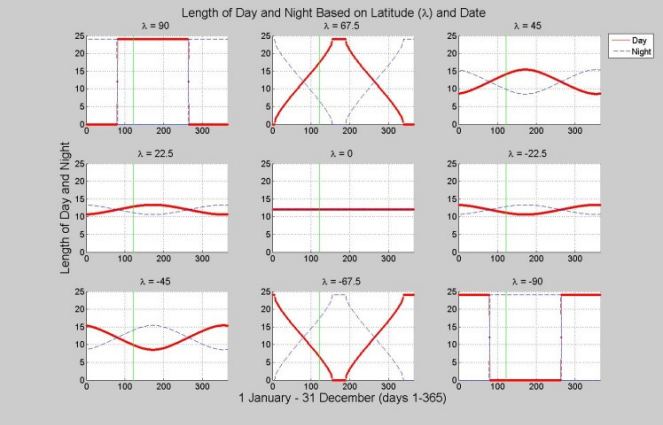

Figure 3. Duration of Daytime and Nighttime for an Entire Year for Various Latitudes l (Vertical green line represents the date May 2, 2012)

The duration of daytime was used in computing the efficiency of reduced-degree-of-freedom solar tracking systems in the next section.

Efficiency of Solar Tracking Systems with Reduced Degree of Freedom

In some applications, the efficiency of the solar panels is traded for the lower cost of the tracking system. Single-axis trackers are widely used in lieu of dual-axis trackers. The single axis can be horizontal, vertical or tilted. Using the model developed in this study, an estimation of the efficiency of these single-axis trackers can be computed when the engineers need to evaluate the trade-offs.

The solar panel efficiency due to sunlight incident angles is the only concern here. The efficiency due to incident angles of solar panels with reduced degrees of freedom is defined to be the ratio of the energy flux per unit area per day of such a solar panel to the energy flux per unit area per day

of dual-axis full solar tracker. Do not confuse this efficiency definition with efficiency of photoelectric energy conversion, which in general is less than 40%. The numerical values of the efficiency due to sunlight incident angles are much higher, but this fact does not imply any contradiction. This efficiency may vary each day in the year, but what is of particular interest is the annual average, or the seasonal average, of the efficiency. It may vary with local latitude as well. The efficiency in numerical values for New York City, as an example, which has latitude λ = 40º47', is calculated throughout this analysis. At the end of this section, the efficiencies are compared with two other locations with different latitudes, Los Angeles, CA, and Miami, FL. With this analysis, it makes it easier to estimate quantitatively how much gain in power the full tracking system may obtain compared to less-expensive partial tracker systems or even seasonally adjusted fixed solar panels. This will assist with the decision-making process on the difference choices of solar panel systems in the investment and installation of such systems.

Efficiency of Seasonally Adjusted Fixed Panel Systems

One simple improvement related to efficiency, on top of the fixed solar panels, is to seasonally adjust the tilt angle of the solar panel manually. Solar panels with dual-axis trackers and with programmed active drives, as discussed in the last section, are able to guarantee the orthogonal incident of sunlight all the time and are the most efficient. The seasonally adjusted fixed panel systems are always oriented to face due south. In the spring and fall, the tilt angle is adjusted to face the celestial equator, with an altitude angle λ, which is the local latitude.

For six months of the year, the duration of daylight is longer than 12 hours. However, the usable time for the incident sunlight is truncated at 12 hours because the sun is behind the panel for the rest of the day. For the other six months, the duration of daylight is less than 12 hours. So for three months in the summer, the incident sunlight is 12 hours long. For spring and fall there are one and half months with 12 hours of sunlight and one and half months with less than 12 hours. For winter, it is always less than 12 hours.

Summer

Assume that in summer the panel tilt is adjusted to a declination angle $\bar{\sigma} = \frac{3\varepsilon}{4}$. The average incident angle is taken as $\frac{\varepsilon}{8}$. In the three months of summer, the sunlight is longer than 12 hours. While a full tracker can take advantage of this fact, the fixed panel has to truncate the sunlight to 12 hours. The fixed panel only makes use of a portion of sunlight during the day, which is $\frac{12}{\bar{d}}$, where $\bar{d}$ is the average duration of daytime.

$$\bar{d} = 24[1 - (\cos^{-1}(\tan(\frac{3\varepsilon}{4}).\tan\lambda))/\pi] \tag{16}$$

The efficiency for summer is, then,

$$\frac{12}{\bar{d}}(\cos\frac{\varepsilon}{8})\frac{1}{\pi}\int_{-\frac{\pi}{2}}^{\frac{\pi}{2}}\cos\varphi d\varphi \tag{17}$$

The efficiency varies with local latitude because the average duration of daylight depends on the latitude. For New York City, for example, with the latitude λ = 40º47', the efficiency is 53.97%.

Spring and Fall

For spring or fall, the solar panel is adjusted to aim at the vernal equinox or autumnal equinox, thus the efficiency for spring and fall is the same, due to symmetry. Here, only the analysis for the spring is described.

For the 1.5 months of spring with more than 12 hours of daylight, the average duration of daylight is

$$\bar{d} = 24[1 - (\cos^{-1}(\tan(\frac{\varepsilon}{4}).\tan\lambda))/\pi] \tag{18}$$

The efficiency can be approximated by

$$\frac{12}{\bar{d}}(\cos\frac{\varepsilon}{4})\frac{1}{\pi}\int_{-\frac{\pi}{2}}^{\frac{\pi}{2}}\cos\varphi d\varphi \tag{19}$$

For New York City, with the latitude λ = 40º47', in this period, the efficiency is 59.7%.

For the other 1.5 months of spring, the average duration of daylight must be considered, which depends on the local latitude. For the first-order approximation, take the average declination as

$$\bar{\sigma} = -\frac{\varepsilon}{4} \tag{20}$$

The efficiency of the solar panel for these 1.5 months is

$$(\cos\frac{\varepsilon}{4})\frac{1}{\pi}\int_{-\frac{\pi}{2}}^{\frac{\pi}{2}}\cos\varphi d\varphi \tag{21}$$

which has a numerical value of 63.3%. The overall average efficiency for spring and fall is 61.5%.

Winter

During the three winter months, the daylight time is less than 12 hours. Take the average declination as

$$\overline{\sigma} = -\frac{3\varepsilon}{4} \tag{22}$$

and the average incident angle of sunlight as $\frac{\varepsilon}{8}$.

The solar panel efficiency for winter is approximately

$$(\cos\frac{\varepsilon}{8})\frac{1}{\pi}\int_{-\frac{\pi}{2}}^{\frac{\pi}{2}}\cos\varphi d\varphi \tag{23}$$

which is calculated to be 63.6% for New York City.

Efficiency of Horizontal Single Axis Trackers (HSAT)

HSAT trackers have horizontal axes. These trackers are able to follow the altitude of the sun but not the azimuth from east to west. There is limited improvement from seasonally adjusted fixed panels. They suffer in the same way as fixed panels in the summer and half of spring and half of fall to utilize the periods of longer than 12 hours of sunlight. The efficiency in winter is

$$\frac{1}{\pi}\int_{-\frac{\pi}{2}}^{\frac{\pi}{2}}\cos\varphi d\varphi \tag{24}$$

which is 63.7%.

The efficiency in the summer is

$$\frac{12}{\overline{d}}\frac{1}{\pi}\int_{-\frac{\pi}{2}}^{\frac{\pi}{2}}\cos\varphi d\varphi \tag{25}$$

The average daylight is the same in summer

$$\overline{d} = 24[1-(\cos^{-1}(\tan(\frac{3\varepsilon}{4}).\tan\lambda))/\pi] \tag{26}$$

For New York City, with a latitude λ = 40º47', the efficiency turns out to be 54.0%.

For half of the spring, which is right before summer, the average daylight time is

$$\overline{d} = 24[1-(\cos^{-1}(\tan(\frac{\varepsilon}{4}).\tan\lambda))/\pi] \tag{27}$$

and the efficiency is 60.2%. The average efficiency for the other half of the spring, which is immediately after winter, is 63.7%. The overall efficiency for spring or fall is, then, 62.0%.

Efficiency of Tilted Single Axis Trackers (TSAT)

In these trackers, the axis is tilted so that at noon the panel is facing the intersection of the celestial equator on the local meridian. The panel rotates daily from east to west to follow the sun. The incident angle is fixed for each day and is the same as the solar declination angle σ. The annual average efficiency for this TSAT is

$$\frac{1}{2\varepsilon}\int_{-\varepsilon}^{\varepsilon}\cos\sigma d\sigma \tag{28}$$

which is independent of the local latitude and has a value of 97.2%.

Efficiency of Vertical Single Axis Trackers (VSAT)

VSAT trackers can rotate along a vertical axis and follow the sun from east to west daily. These tracers make full use of longer daytime during the summer. Suppose the panel is optimally oriented in such a way that it faces the celestial equator at noon, the efficiency of VSAT trackers would be calculated as

$$\frac{1}{\varepsilon}\int_{0}^{\varepsilon}\frac{1}{2\alpha+\sigma}\int_{-\alpha}^{\alpha+\sigma}\cos\theta d\theta d\sigma \tag{29}$$

where $\alpha = \frac{\pi}{2} - \lambda$ is the co-latitude.

This can be approximated as

$$\frac{1}{\alpha}\int_{0}^{\alpha}\cos\theta d\theta \tag{30}$$

resulting in an efficiency of 88.2% for New York City.

The efficiencies for two other cities, Los Angeles, CA, and Miami, FL, are calculated and compared in the following tables. Los Angeles has a latitude λ = 34º03', and Miami has a latitude of λ = 25º46'.

Table 1. Efficiencies for Seasonally Adjusted Fixed panels

	SAF summer	SAF spring or fall	SAF winter
New York	54.0%	61.5%	63.6%
Los Angeles	55.9%	62.0%	63.6%
Miami	57.8%	62.3%	63.6%

Table 2. Efficiencies for Horizontal Single Axis Trackers

	HSAT summer	HSAT spring or fall	HSAT winter
New York	54.0%	62.0%	63.7%
Los Angeles	56.0%	62.4%	63.7%
Miami	57.9%	62.7%	63.7%

Table 3. Efficiencies for Tilted Single Axis Trackers and Vertical Single Axis Trackers

	TSAT	VSAT
New York	97.2%	88.2%
Los Angeles	97.2%	84.8%
Miami	97.2%	80.5%

Conclusions

The analysis of the diurnal motion of the sun on the celestial sphere using a geocentric model was used for an active dual-axis solar tracker in order to optimize the incident angle and, hence, optimize the received energy flux from the sunlight. The numerical values of the declination angles and azimuthal angles of the sun, sunrise, sunset time, and duration of daytime for any date in the year, and conducted simulations for various locations with different latitude and dates in a year were calculated. Solar panel efficiency due to incident angles for restricted-degree-of-freedom solar trackers for different seasons and the annual average were also analyzed. The results indicated that the tilted single-axis trackers (TSAT) have the highest efficiency, which is independent of the local latitude. The horizontal single-axis trackers do not offer significant improvements over the seasonally adjusted fixed panels. This analysis has significance in providing guidance in the decision-making process of initially installing a solar panel system. In summary, this paper presents not only a visual tool but also a computational tool to assist engineers and consumers in their decision making for investment in appropriate solar panels and tracking systems in terms of trade-offs for energy maximization in their particular applications.

References

[1] Green, M. A., Emery, K., Hishikawa, Y., & Warta W. (2009). Solar Cell Efficiency Tables (Version 34). *Progress in Photovoltaics: Research and Applications,* 17, 320–326. (Published online in Wiley InterScience (www.interscience.wiley.com) DOI: 10.1002/pip.911)

[2] Ning, K., Chen, J., Yu, T., Zhou, G., Chen, X., & Yu, G. (2011). Design of the Attitude Automatic Adjusting System for the Solar Panel. *Proceedings of the 2011 IEEE 2nd International Conference on Computing, Control and Industrial Engineering (CCIE),* (pp. 367-370). (dio: 10.1109/CCIENG.2011.6008035)

[3] Chen, Y. M., & Wu, H. C. (2001). Determination of the Solar Cell Panel Installation Angle. *Proceedings of the 2001 4th IEEE International Conference on Power Electronics and Drive Systems,* (pp. 549-554).

[4] Mokhtari, B., Ameur, A., Mokrani, L., Azoui, B., & Benkhoris, M. F. (2009). DTC Applied to Optimize Solar Panel Efficiency. *Proceedings of the 35th Annual IEEE Conference on Industrial Electronics*, *IECON '09*, (pp. 1122-1127). (doi: 10.1109/IECON.2009.5414681)

[5] Oltu, O., Milea, P. L., Dragulinescu, M., & Franti, E. (2007). Solar Panel Energetic Efficiency Optimization Method, Based on a Specific Detector and Orientation Microsystem. *Proceedings of the IEEE International Semiconductor Conference, CAS 2007,* (pp. 127-130).

[6] Rizk, J., & Chaiko, Y. (2008). Solar Tracking System: More Efficient Use of Solar Panels. *World Academy of Science, Engineering and Technology*, 41, 313-315.

[7] Li, D. H.W., & Lam, T. N. T. (2007). Determining the Optimum Tilt Angle and Orientation for Solar Energy Collection Based on Measured Solar Radiance Data. *International Journal of Photoenergy*, Article ID 85402, 1-9 (doi:10.1155/2007/85402)

[8] Xu, J., Wu, K., & Ma, L. (2009). All-Weather Automatic Solar Tracking Method Applied in Forest Fire Prevention. *Proceedings of the 9th International Conference on Electronic Measurement & Instruments, ICEMI'2009,* (pp. 1-805 – 1-809).

[9] Kuo, J. L., Chao, K. L., & Lee, L. S. (February 2010). Dual Mechatronic MPPT Controllers with PN and OPSO Control Algorithms of the Rotatable Solar Panel in PHEV System. *IEEE Trans. Industrial Electronics,* 57(2), 678-689.

[10] Chen, Y. M., Lee, C. H., & Wu, H. C. (June 2005). Calculation of the Optimum Installation Angle for Fixed Solar-Cell Panels Based on the Genetic Algorithm and the Simulated-Annealing Method. *IEEE Transactions on Energy Conversion,* 20(2), 467-473.

[11] Lu, W. H., & He, X. L. (December 2008). Development of Full-Automatic Solar Tracker and Its Application. *Optics and Precision Engineering*, 16(12), 2544-2550.

[12] Dousoky, G. M., El-Sayed, A. H. M., & Shoyama, M. (2011). Maximizing Energy-Efficiency in single-Axis Solar Trackers for Photovoltaic Panels. *Proceedings of the 8th IEEE International Conference on Power Electronics - ECCE Asia*, (pp. 1458-1463). The Shilla Jeju, Korea.

[13] Chang, Y. (2011). Vehicle Profile Design versus Solar Energy Collection: Styling Considerations for Solar-powered Personal Commuter Vehicles. *International Journal of Engineering Research & Innovation*, 3(1), 15-24.

[14] Soares, A., Li, C. (2011). Using Solar Energy in Robotics and Small-Scale Electronic Applications. *International Journal of Engineering Research & Innovation*, 3(2), 27-30.

[15] Tango, R. W. (2009). Technology Integration into Architecture Building Systems. *Technology Interface International Journal*, 10(2), 1-15.

Biographies

HONGYU GUO is an Assistant Professor of Computer Science at University of Houston – Victoria. He received his Ph.D. degree in Computer Science from the University of Florida. His research interests are in computer vision, simulation and image processing. Dr. Guo may be reached at guoh@uhv.edu.

MEHRUBE MEHRUBEOGLU is an Associate Professor of Mechanical Engineering and Engineering Technology at Texas A&M University-Corpus Christi. She earned her B.S. degree in Electrical Engineering from The University of Texas at Austin, MS degree in Bioengineering from Texas A&M University, and Ph.D. degree in Electrical Engineering from Texas A&M University. Dr. Mehrubeoglu's interests lie in imaging and image processing applications, instrumentation, optical property measurements, and renewable energy. She can be reached at ruby.mehrubeoglu@tamucc.edu.